Corrigendum to Weather Clim. Dynam., 3, 1215–1236, 2022
https://doi.org/10.5194/wcd-3-1215-2022-corrigendum

Corrigendum to "Stratospheric downward wave reflection events modulate North American weather regimes and cold spells" published in Weather Clim. Dynam., 3, 1215–1236, 2022

Gabriele Messori[1,2,3,4], **Marlene Kretschmer**[5], **Simon H. Lee**[6], **and Vivien Wendt**[7,i]

[1]Department of Earth Sciences, Uppsala University, Uppsala, Sweden
[2]Centre of Natural Hazards and Disaster Science (CNDS), Uppsala, Sweden
[3]Department of Meteorology, Stockholm University, Stockholm, Sweden
[4]Bolin Centre for Climate Research, Stockholm, Sweden
[5]Department of Meteorology, University of Reading, Reading, UK
[6]Department of Applied Physics and Applied Mathematics, Columbia University, New York, NY, USA
[7]Institute for Solar-Terrestrial Physics, German Aerospace Center (DLR), Neustrelitz, Germany
[i]previously published under the name Vivien Matthias

Correspondence: Gabriele Messori (gabriele.messori@geo.uu.se)

Published: 18 March 2024

During the computation of the reflection index, we performed an incorrect area weighting. This has led to changes in the days that we include in the reflection events and in particular resulted in four new events and three events which disappear (Fig. 1). Thus, all references to "44 events" or similar phrasings in Messori et al. (2022) should now read "45 events".

While our qualitative conclusions remain unchanged, this correction requires updating several figures and tables in the study, which we provide below. We underscore that the differences from the previously published material are limited. We comment on the individual figures when notable differences emerge. Whenever we stated exact numbers in Messori et al. (2022) with reference to a figure, we provide here both the updated numbers and the original numbers in parentheses for reference.

Finally, we provided an incorrect explanation of the smoothing procedure for our data. The first paragraph in Sect. 2 in Messori et al. (2022) should read as follows. *We base our analysis on data from the European Centre for Medium-Range Weather Forecasts (ECMWF) ERA5 reanalysis (Hersbach et al., 2020). We use daily data covering the period from 1 December 1979 to 31 March 2021 and focus on an extended winter season covering the months of December, January, February, and March (DJFM). Except for the heat flux, all climatologies are defined as the average of a 15 d centred mean of the same calendar days for all years in the dataset. For example, the climatological temperature of 12 December is the average temperature during 5–19 December of all years from 1979 to 2020. Anomalies are then computed as daily deviations from this climatology. For the computation of the stratospheric reflection index, the 15 d smoothing is instead applied to the meridional heat fluxes after averaging over the Siberian and Canadian domains (see Sect. 3 in Messori et al., 2022) but prior to computing the anomalies. For 2 m temperature in the geographical composites, we additionally smooth the anomalies with a 9 d running mean, which gives greater prominence to persistent temperature anomalies. The 2 m temperature anomalies are further linearly detrended using area-mean 2 m land temperature over North America (30–72.5° N, 190–305° E; the same domain as shown in Fig. 4 in Messori et al., 2022).*

With reference to Fig. 2, the corrected text reads as follows. *During days when RI > 1, eddy heat flux averaged over the Canadian domain is instead almost exclusively negative (i.e. $(v'T')_{\mathrm{Can}} < 0$; Fig. 2d), except for 10 d (previously 28 d) in our sample (less than 1 % (previously ~ 1.5 %) of all reflective days).*

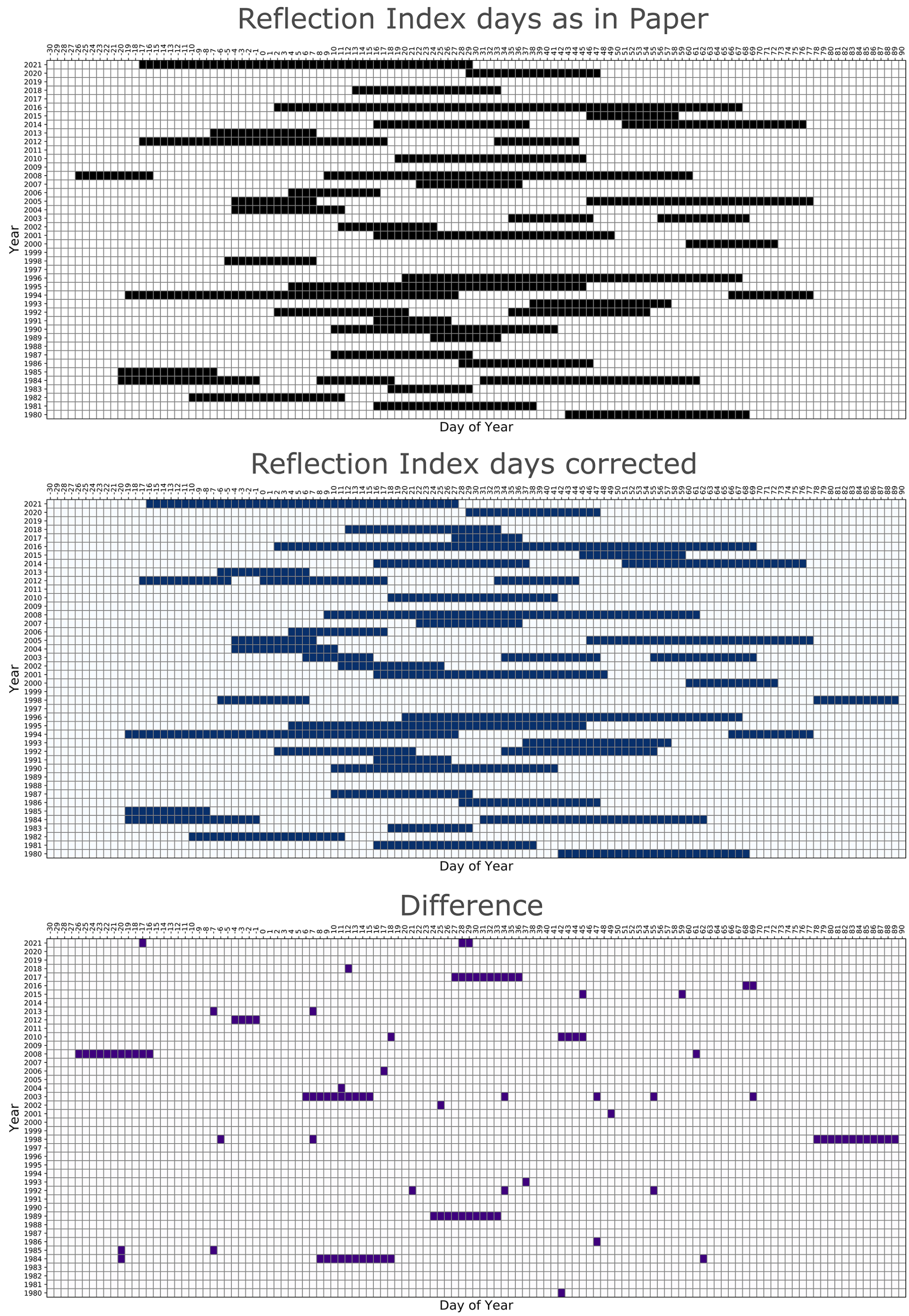

Figure 1. **(a)** Reflection events as used in Messori et al. (2022). **(b)** Corrected reflection events. **(c)** Difference between the two sets of days. The day of year refers to the DJFM season analysed, with 0 being 31 December.

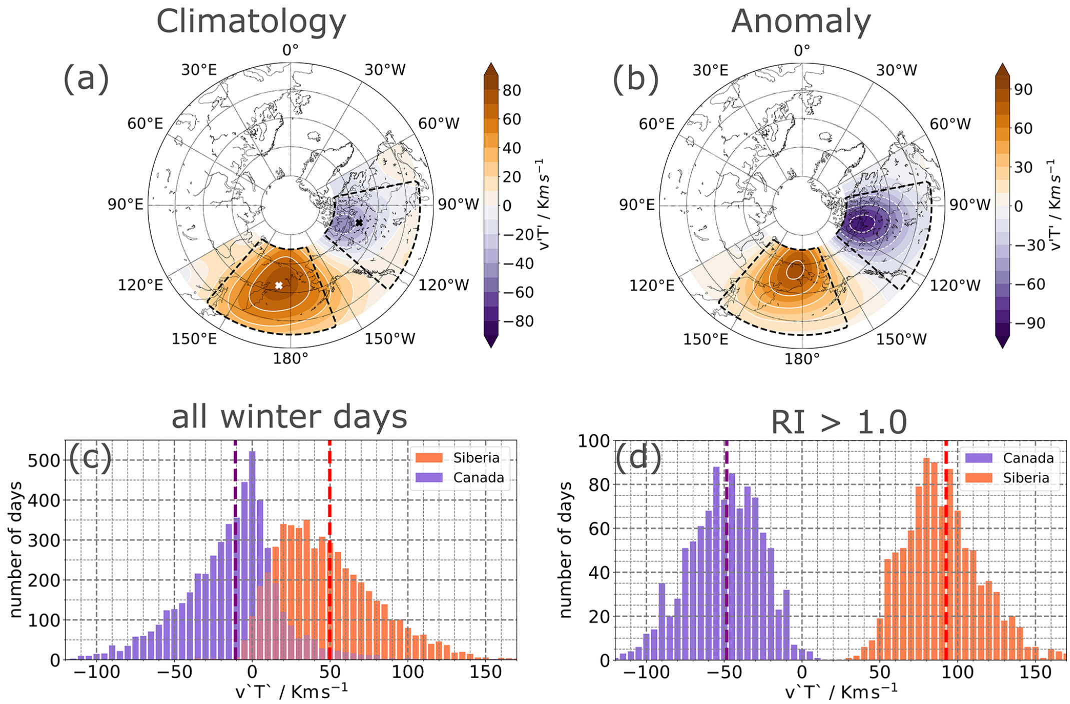

Figure 2. **(a)** Corrected climatology of the wintertime local daily meridional heat flux $v'T'$ at 100 hPa in the Siberian and Canadian sectors. The crosses mark the average centres of mass of the meridional heat flux in the Siberian and Canadian sectors during reflection events. **(b)** Corrected composite anomaly of the local daily meridional heat flux at 100 hPa during reflection events. Corrected histograms of daily meridional heat flux $v'T'$ at 100 hPa averaged for the Canadian (blue) and Siberian (red) sectors for **(c)** all winter days and **(d)** only for days when RI > 1.0. The vertical dashed lines represent the averages over all days. The data cover the DJFM seasons from 1979/1980 to 2020/2021. This figure replaces Fig. 1 in Messori et al. (2022).

With reference to Fig. 4, the corrected text reads as follows. *There is a large spread in the magnitude and persistence of reflection events, with some events lasting more than 4 weeks and reaching RI values of around 6. The median event duration is 19 d (previously 20 d), with a maximum of 68 d (previously 66 d) (event starting 2 January 2016). Whilst the minimum duration is set at 10 d, the average RI in our 45-event sample is significantly greater than 1 for over 2 weeks. We henceforth focus on the 24 d following the reflection event onset, as this both captures the full duration of the typical events and is the maximum lag for which data fall within DJFM for 44 of our 45 events.*

With reference to Fig. 10, the corrected text reads as follows (PT, Pacific Trough; AkR, Alaskan Ridge; ArH, Arctic High; ArL, Arctic Low). *Furthermore, PT to AkR is one of the transitions showing the closest correspondence with wave reflection (Fig. 10b), albeit not significantly more likely than random. The only transitions significantly associated with* RI > 1 *are those into AkR from ArH, as well as the AkR self-transition.*

Finally, we provide corrected text for the following passages in the "Discussion and conclusions" section.

We also analysed whether the reflection events overlap with the occurrence of sudden stratospheric warmings (SSWs) (Table A1), finding that SSWs occur during only 9 of the 45 reflection events. An additional four (previously three) reflection events are preceded by an SSW within 20 d of their onset. Of the nine events coinciding with an SSW, five do not show a substantial drop in surface temperature anomalies over the cold spell domain we analyse here; i.e. they are "warm" or "neutral" events. Moreover, in only three of these nine events does an SSW occur within the first 15 d, which are the lags on which our analysis focuses (and of these, none occur within the first 9 d).

In agreement with the strengthened stratospheric polar vortex observed during the reflection events, we find that reflection events preferentially occur during the westerly phase of the Quasi-Biennial Oscillation (QBOw). Specifically, 33 (previously 30) of the 45 (previously 44) reflection events have an onset during a QBOw month, and 32 (previously 31) peak during a QBOw month.

For example, the stratospheric reflection events occurring on 4 January 1995 and 15 December 2020 (previously 14 December 2020) progress in the opposite sense, from an Alaskan Ridge to a Pacific Trough.

At the same time, PT is the most frequent regime (31.6 % of DJFM days) and thus far more common than reflection *events (which account for roughly (previously just under) 20 % of DJFM days).*

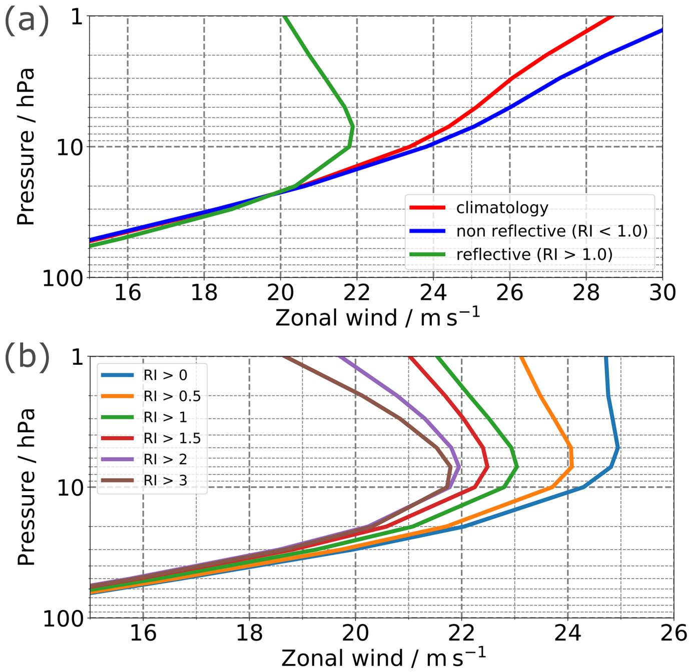

Figure 3. Corrected vertical zonal-mean zonal wind profiles (averaged over 60–80° N) in the stratosphere. **(a)** Climatology of all winter days (red line), days when RI > 1 (green line), and days when RI < 1 (blue line). **(b)** Same as **(a)**, but for days when RI exceeds different thresholds. This figure replaces Fig. 2 in Messori et al. (2022).

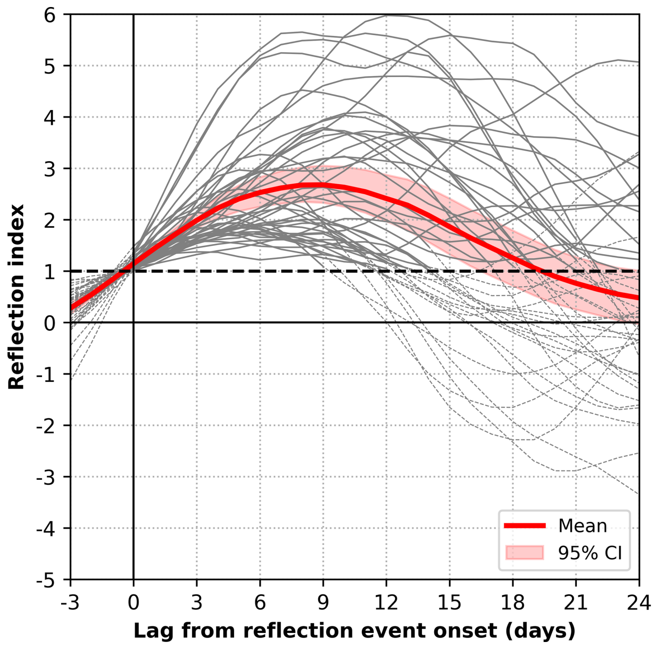

Figure 4. Corrected evolution of the reflection index (grey lines) for the 45 identified reflection events (i.e., RI > 1 for at least 10 consecutive days) as a function of days from event onset. Lines are dashed where the threshold is not met. The thick red line denotes the average over all events, and the horizontal dashed black line indicates the threshold of RI = 1. Shading indicates a 95 % confidence interval on the mean, assessed as described in Sect. 2 in Messori et al. (2022). This figure replaces Fig. 3 in Messori et al. (2022).

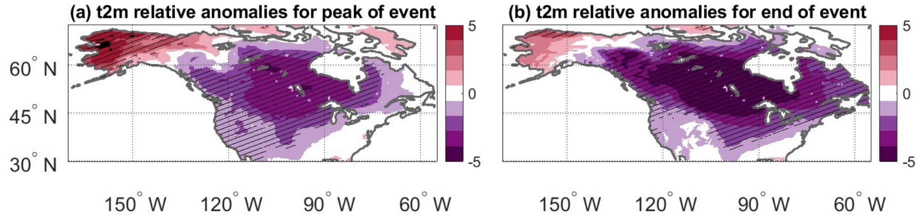

Figure 5. Corrected composite 2 m temperature (t2m) anomalies (K) relative to onset of reflection events for **(a)** the peak and **(b)** the end of all reflection events. Hatching denotes statistically significant anomalies, assessed as described in Sect. 2 in Messori et al. (2022). This figure replaces Fig. 4c and d in Messori et al. (2022).

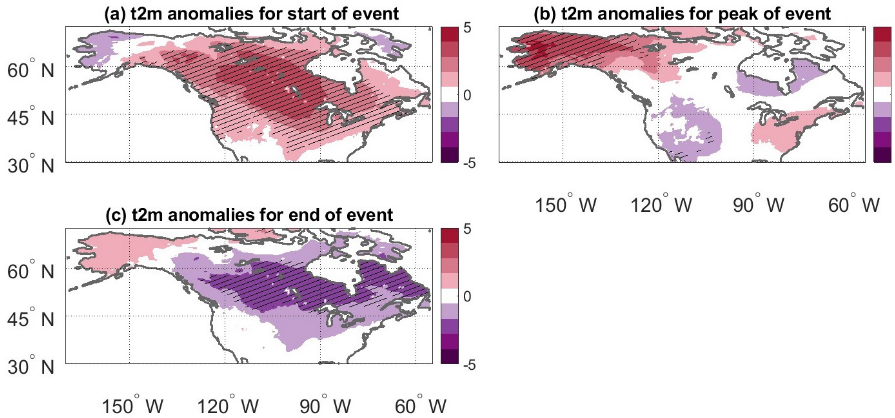

Figure 6. Corrected composite-mean 2 m temperature (t2m) anomalies at the **(a)** onset, **(b)** peak, and **(c)** end of the reflection events. Hatching denotes statistically significant anomalies, assessed as described in Sect. 2 in Messori et al. (2022). This figure replaces Fig. 5 in Messori et al. (2022).

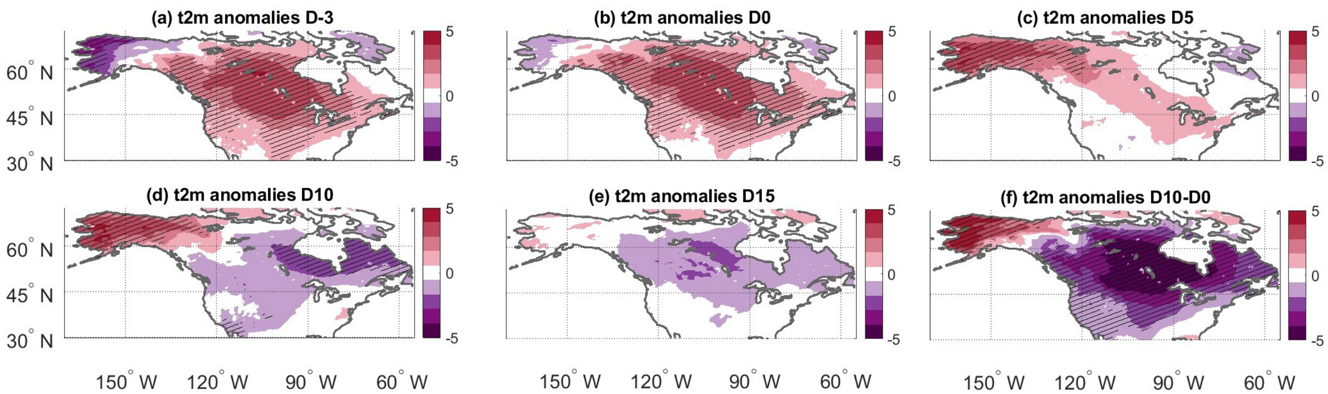

Figure 7. Corrected composite-mean 2 m temperature (t2m) anomalies at various lags relative to the reflection event onset. **(f)** Average difference between the t2m anomalies on day 10 and day 0 (i.e. **d**–**b**). Hatching denotes statistically significant anomalies, assessed as described in Sect. 2 in Messori et al. (2022). This figure replaces Fig. 6 in Messori et al. (2022).

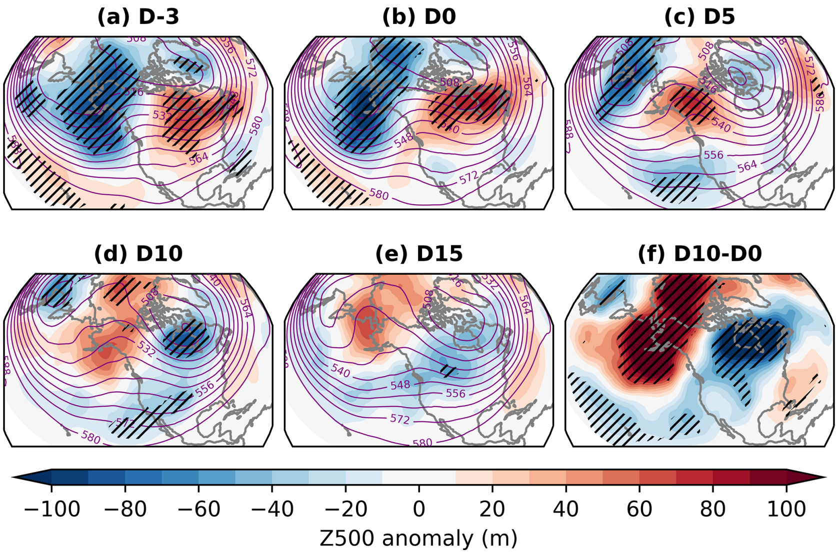

Figure 8. (a–e) Corrected composite-mean 500 hPa geopotential height (Z_{500}) (purple contours, dam) and anomalies (shading, m) at various lags relative to the reflection event onset. **(f)** Corrected average difference between the Z_{500} anomalies on day 10 and day 0 (i.e. **d**–**b**). Hatching denotes statistically significant anomalies, assessed as described in Sect. 2 in Messori et al. (2022). This figure replaces Fig. 7 in Messori et al. (2022).

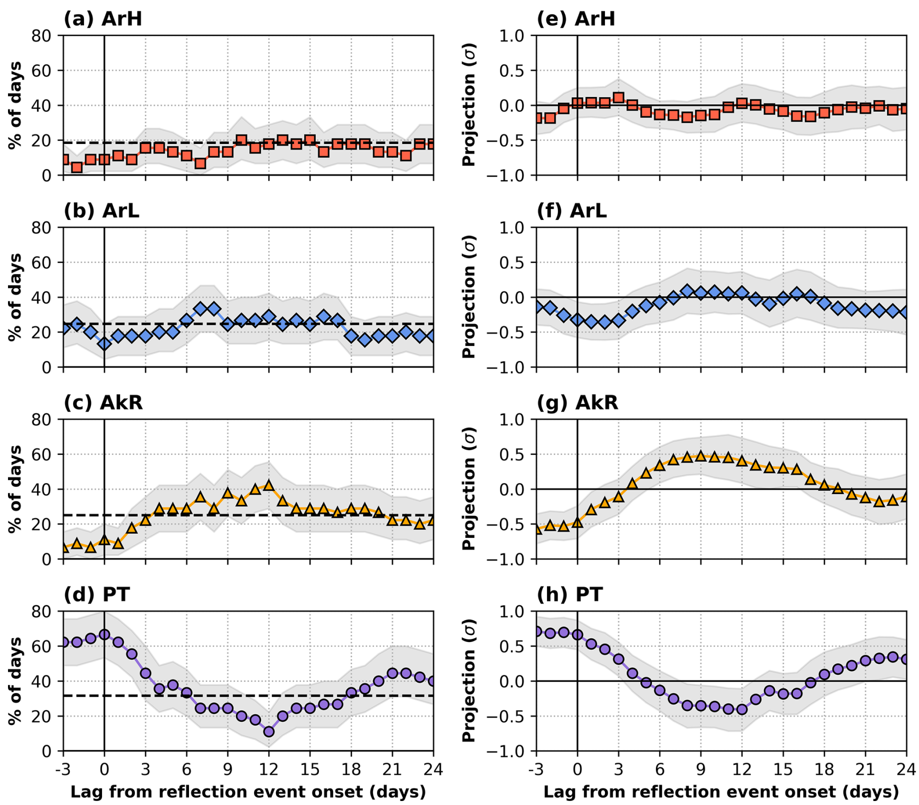

Figure 9. (a–d) Corrected proportion of days in the 45-event sample assigned to each regime. The horizontal dashed lines indicate the climatological DJFM frequency of each regime. **(e–h)** Corrected mean normalised projection onto each regime for the 45 events. Grey shading indicates 95 % confidence intervals assessed as described in Sect. 2 in Messori et al. (2022). This figure replaces Fig. 8 in Messori et al. (2022).

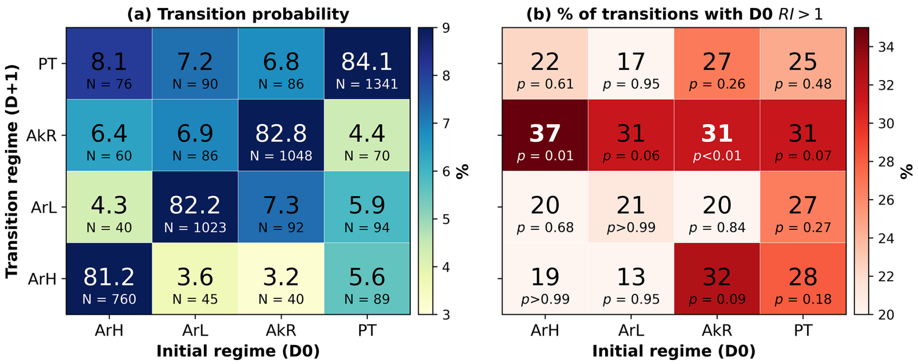

Figure 10. **(a)** Corrected transition matrix for the four North American weather regimes. For each initial regime (x axis), the numbers in each column denote the observed probability (expressed as a percentage; columns sum to 100) of persisting in the same regime (white font) or transitioning into a different regime. The total number of instances of each transition (N) is also shown. **(b)** Corrected percentage of each transition pathway which occurs with RI > 1 on the day prior to the transition (D0), expressed as percentages. P values indicate the estimated probability of obtaining a statistic greater than the observed value by chance, assessed by randomly re-sampling all DJFM days 10 000 times (without replacement) using the observed sample sizes for each transition pathway. Statistics significant at the one-sided 5 % significance level are in bold white font. This figure replaces Fig. 9 in Messori et al. (2022).

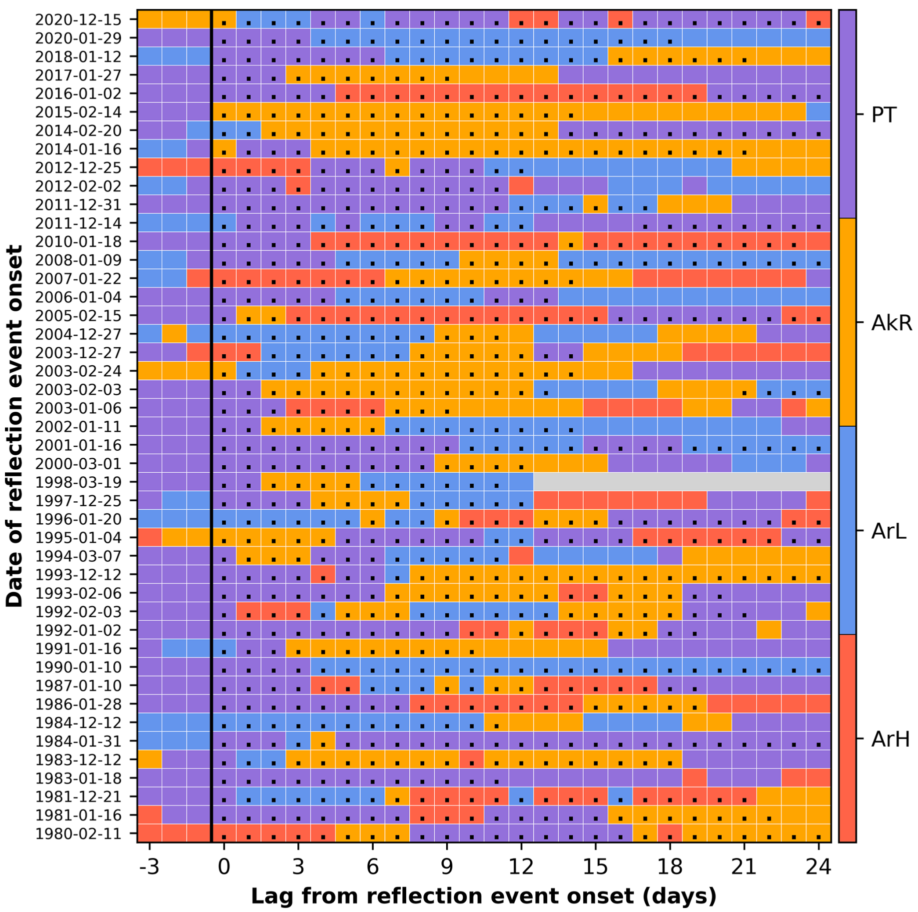

Figure 11. Corrected evolution of the daily regime assignment during the 45 reflection events. Days with RI > 1 are shown with dots. Days beyond 31 March are shown in grey. This figure replaces Fig. 11 in Messori et al. (2022).

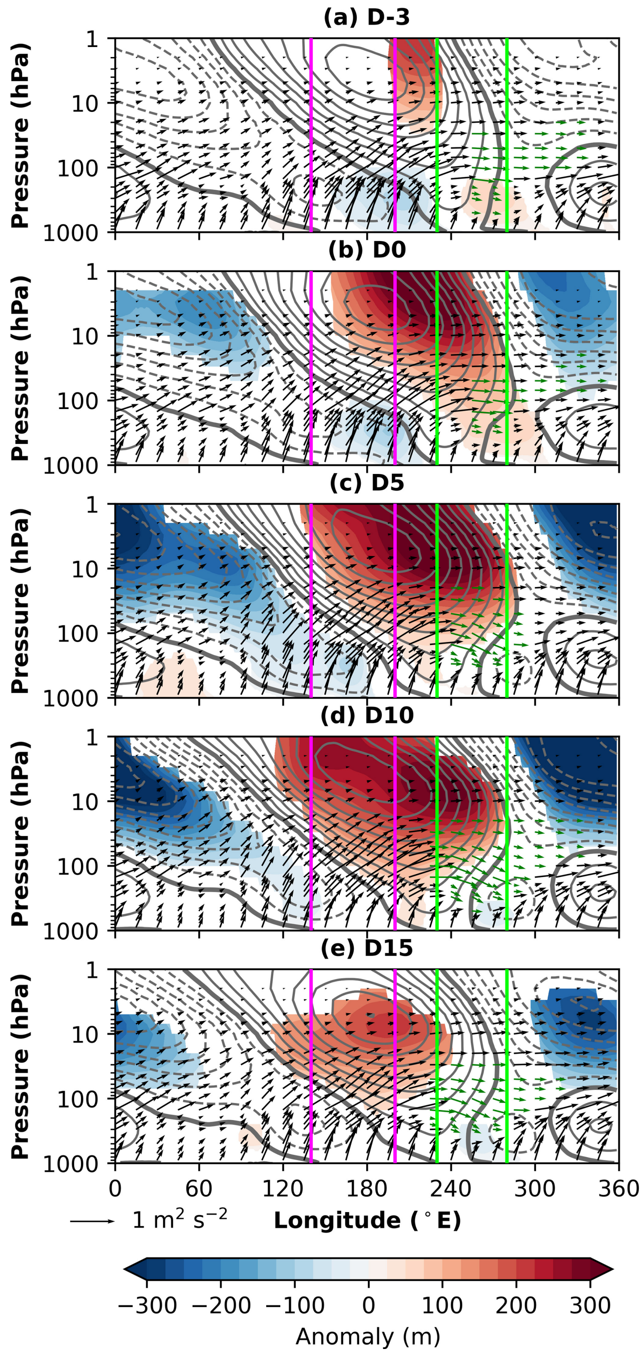

Figure 12. Corrected evolution of the mean vertical wave structure associated with reflection events. Grey contours denote the average 40–80° N eddy geopotential height field (contours every 100 m, dashed negative, zero contour thickened). Shading denotes significant departures of the eddy height field from climatology, with significance assessed as described in Sect. 2. Vertical pink lines delineate the longitudinal range of the Siberian box (140–200° E), and vertical green lines delineate the longitudinal range of the Canadian box (230–280° E). Arrows denote the vertical and zonal components of the 40–80° N average Plumb wave activity flux, calculated over wavenumbers 1–3 (Plumb, 1985). Green arrows indicate the vertical component is downward. Arrows are scaled following Millin et al. (2022). This figure replaces Fig. 12 in Messori et al. (2022).

Appendix A: Additional tables and figures

Table A1. Corrected onset and end dates, temperature classification, and SSW coincidence for the 45 selected stratospheric reflection events. An SSW is considered to coincide with a reflection event if the dates of the two events overlap. We used the SSW catalogue from NOAA Chemical Sciences Laboratory (2020) and the additional event described in Lee (2021). For the SSWs in NOAA Chemical Sciences Laboratory (2020) only those present in at least two reanalysis products were counted. This table replaces Table A1 in Messori et al. (2022).

Event no.	Onset date	End date	Class	SSW
1	11 Feb 1980	9 Mar 1980	Neutral	Y
2	16 Jan 1981	7 Feb 1981	Warm	N
3	21 Dec 1981	11 Jan 1982	Cold	N
4	18 Jan 1983	29 Jan 1983	Warm	N
5	12 Dec 1983	30 Dec 1983	Cold	N
6	31 Jan 1984	3 Mar 1984	Warm	Y
7	12 Dec 1984	23 Dec 1984	Cold	N
8	28 Jan 1986	16 Feb 1986	Warm	N
9	10 Jan 1987	29 Jan 1987	Cold	Y
10	10 Jan 1990	10 Feb 1990	Warm	N
11	16 Jan 1991	26 Jan 1991	Cold	N
12	2 Jan 1992	21 Jan 1992	Cold	N
13	3 Feb 1992	24 Feb 1992	Cold	N
14	6 Feb 1993	26 Feb 1993	Cold	N
15	12 Dec 1993	27 Jan 1994	Cold	N
16	7 Mar 1994	18 Mar 1994	Cold	N
17	4 Jan 1995	14 Feb 1995	Warm	N
18	20 Jan 1996	8 Mar 1996	Cold	N
19	25 Dec 1997	6 Jan 1998	Cold	N
20	19 Mar 1998	30 Mar 1998	Warm	N
21	1 Mar 2000	13 Mar 2000	Cold	N
22	16 Jan 2001	17 Feb 2001	Neutral	Y
23	11 Jan 2002	25 Jan 2002	Cold	N
24	6 Jan 2003	15 Jan 2003	Cold	N
25	3 Feb 2003	16 Feb 2003	Cold	N
26	24 Feb 2003	10 Mar 2003	Cold	N
27	27 Dec 2003	10 Jan 2004	Cold	Y
28	27 Dec 2004	7 Jan 2005	Warm	N
29	15 Feb 2005	18 Mar 2005	Cold	N
30	4 Jan 2006	17 Jan 2006	Warm	N
31	22 Jan 2007	5 Feb 2007	Cold	N
32	9 Jan 2008	2 Mar 2008	Cold	Y
33	18 Jan 2010	10 Feb 2010	Cold	Y
34	14 Dec 2011	26 Dec 2011	Warm	N
35	31 Dec 2011	17 Jan 2012	Warm	N
36	2 Feb 2012	13 Feb 2012	Cold	N
37	25 Dec 2012	6 Jan 2013	Warm	Y
38	16 Jan 2014	6 Feb 2014	Cold	N
39	20 Feb 2014	17 Mar 2014	Cold	N
40	14 Feb 2015	28 Feb 2015	Cold	N
41	2 Jan 2016	10 Mar 2016	Cold	N
42	27 Jan 2017	5 Feb 2017	Cold	N
43	12 Jan 2018	2 Feb 2018	Warm	N
44	29 Jan 2020	16 Feb 2020	Cold	N
45	15 Dec 2020	27 Jan 2021	Warm	Y

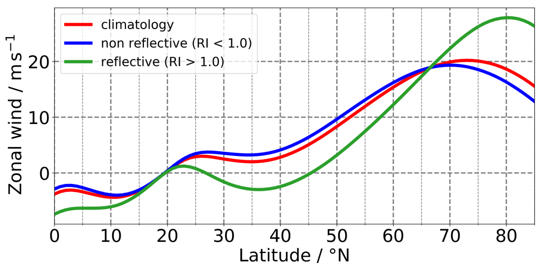

Figure A1. Corrected meridional profiles of the zonal wind averaged over 230–280° E (Canadian sector) at 30 hPa. Climatology of all winter days (red line), days when RI > 1 (green line), and days when RI < 1 (blue line). This figure replaces Fig. A2 in Messori et al. (2022).

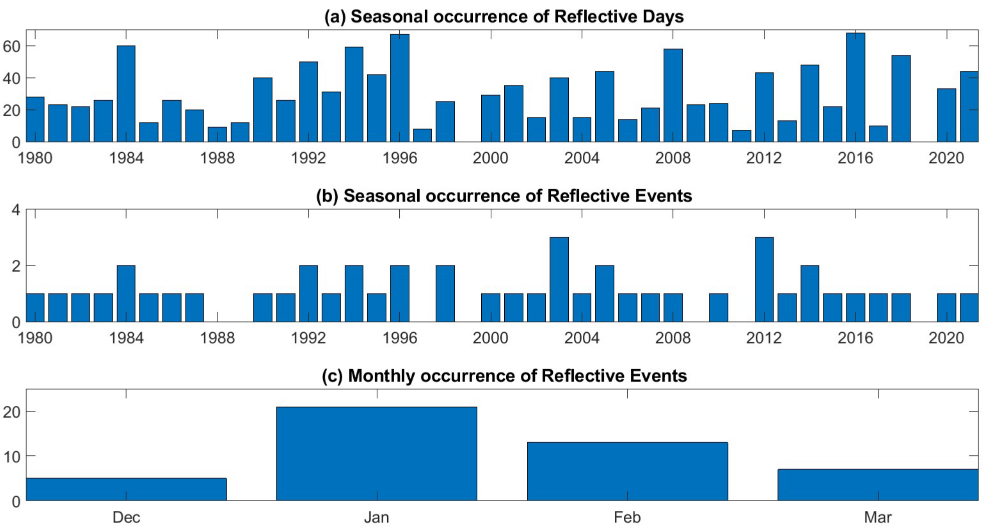

Figure A2. Corrected seasonal occurrence of reflective days (RI > 1.0) **(a)** and seasonal **(b)** and monthly **(c)** occurrence of stratospheric reflection events from December 1979 to March 2021. For reflection events, the date of maximum RI is used. This figure replaces Fig. A3 in Messori et al. (2022).

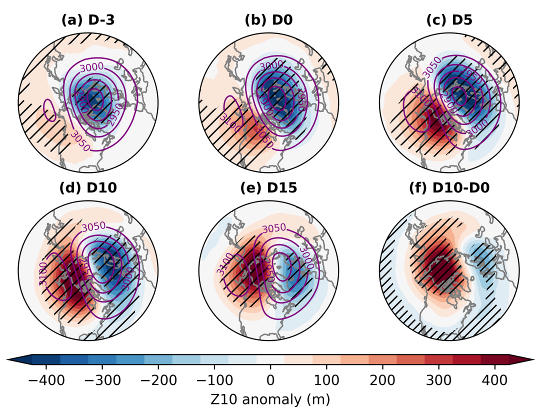

Figure A3. (a–e) Corrected composite-mean 10 hPa geopotential height (Z_{10}, contours, dam) and Z_{10} anomalies (shading, m) at various lags relative to the reflection event onset. **(f)** Corrected average difference between the Z_{10} anomalies on day 10 and day 0 (i.e. **d**–**b**). Hatching denotes statistically significant anomalies, assessed as described in Sect. 2 in Messori et al. (2022). This figure replaces Fig. A4 in Messori et al. (2022).

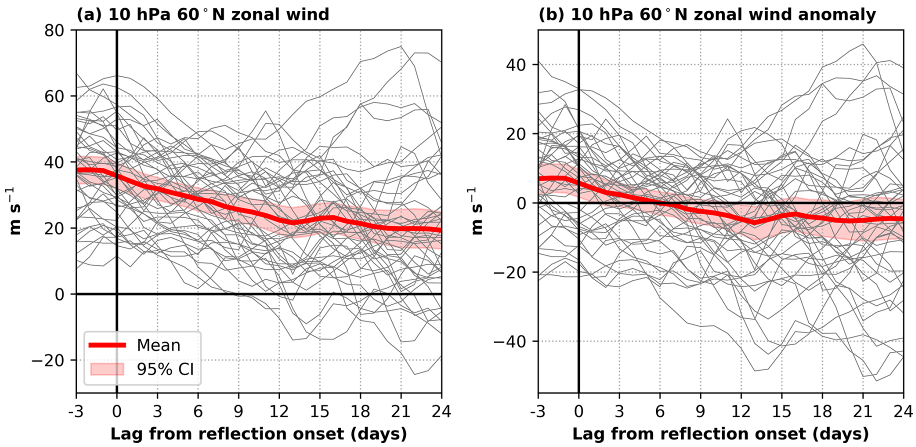

Figure A4. Corrected evolution of the 10 hPa 60° N zonal-mean zonal wind **(a)** and anomalies **(b)** for the 45 reflection events. The thick red line denotes the average over all events. Red shading indicates the 95 % confidence interval on the mean, assessed as described in Sect. 2 in Messori et al. (2022). This figure replaces Fig. A5 in Messori et al. (2022).

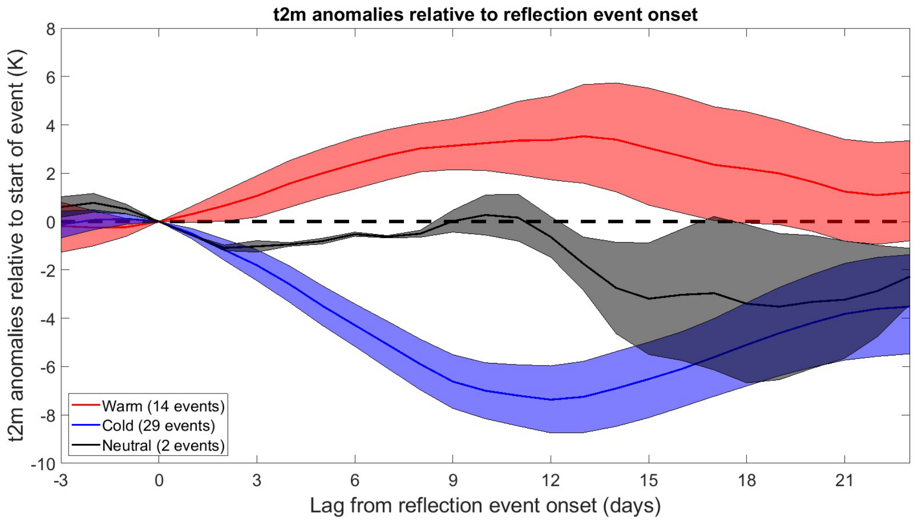

Figure A5. Corrected composite-mean t2m anomalies (K) relative to onset of the reflection events for warm (red), cold (blue), and neutral (black) events. These classes of events are defined according to the area-averaged t2m anomaly over 40–55° N and 260–290° E 10 d after onset: cold events (29, previously 28) have an anomaly < -0.5 K; warm events (14, previously 12) have an anomaly $> +0.5$ K. Events with anomalies between $+0.5$ and -0.5 K are termed neutral (two, previously four). Shading indicates 95% confidence intervals, assessed as described in Sect. 2 in Messori et al. (2022). Due to the small sample size, the confidence interval for neutral events should be interpreted with care. This figure replaces Fig. A7 in Messori et al. (2022).